ISSN 1027-5495. Functional Materials, 24, No.4 (2017), p. 621-627.
doi:https://doi.org/10.15407/fm24.04.621

Fluctuations of ionizing particle track structure and energy resolution of scintillators

***A.V.Gektin*[1], *A.N.Vasil'ev*[2]**

[1]Institute for Scintillation Materials, STC"Institute for Single Crystals", National Academy of Sciences of Ukraine, 60 Nauki Ave., 61001 Kharkiv, Ukraine
[2]Skobeltsyn Institute of Nuclear Physics of Lomonosov Moscow State University, 1(2) Leninskie Gory, 119991 Moscow, Russia

Received August 1, 2017

The work is devoted to the study of fluctuations in ionizing particle track to the energy resolution deterioration. Reasons of deterioration of energy resolution of scintillators due to relatively rare events of production of high-energy Auger and delta-electrons are discussed in terms of different decay from regions with different concentration of excitations in track region. The model allows to assume that decay time changes reflect track non-uniformity and following energy resolution changes. The shallow traps which change the mobility of charge carriers could influence the long components of the decay and therefore modify the input to scintillation signal from regions with low concentration of excitations. This effect could be significant in deterioration of energy resolution of scintillators.

Keywords: Ionizing particle track, energy resolution, scintillators.

Работа посвящена изучению влияния флуктуаций в треке ионизирующей частицы на изменение энергетического разрешения сцинтиллятора. Причины ухудшения энергетического разрешения сцинтилляторов из-за относительно редких генераций высокоэнергетических Оже и дельта-электронов обсуждаются в терминах различий кинетики затуханий из областей с разной концентрацией возбуждений в области трека. Модель предполагает, что изменения времени затухания связаны с флуктуациями распределения плотности возбуждений от трека к треку, что приводит к ухудшению энергетического разрешения. Мелкие ловушки, которые изменяют подвижность носителей заряда, могут влиять на длинные компоненты времени затухания и, следовательно, изменять сцинтилляционный отклик в областях с низкой концентрацией возбуждений. Этот эффект может быть существенным для ухудшения энергетического разрешения сцинтилляторов.

Флуктуації структури треку іонізуючої частинки і енергетичне розділення сцинтиляторів. *О.В.Гектін, А.М.Васильєв.*

Робота присвячена вивченню флуктуацій у треку іонізуючої частинки на погіршення енергетичного розділення сцинтилятора. Причини погіршення енергетичного розділення сцинтиляторів через відносно рідкісні генерації Оже і дельта-електронів обговорюються в термінах відмінностей розпадів із областей з різною концентрацією збуджень у області треку. Модель дозволяє припустити, що зміни часу загасання відображають неоднорідності треку і подальші зміни енергетичного розділення. Дрібні пастки, які змінюють рухливість, можуть впливати на довгі компоненти часів загасання і, отже, змінювати сцинтиляційний відгук в областях з низькою концентрацією збуджень. Цей ефект може бути суттєвим у погіршенні енергетичного розділення сцинтиляторів.

1. Introduction

Non proportionality (NP) of scintillation response is usually used as an explanation of intrinsic resolution change, nevertheless there are no direct links between definitions of these scintillation parameters. At [1] the wide spread between light yield (LY) and energy resolution (ER) was pointed for the same scintillator (NaI:Tl). The literature data are between 5 and 12 % resolution that is out of the LY spread! It is important to note that NP significantly depends on crystal purity, co-doping, integration time and so on [2, 3]. In other words it is necessary to assume that ER depends on the scintillator structure as well nevertheless there are no any "structure parameters" in ER definition (only statistical parameters).

These experimental data allow to assume that not all scintillation events have the same contribution to the PMT registered statistics, and it is necessary to find the core for such difference. Moreover, the decay kinetics also fluctuates significantly. These two factors approve the supposition that the main reason for such effects is the fluctuation of spatial distribution of electrons, holes and activators in the track region. In order to demonstrate this link we analyze the distribution of electron and hole concentrations just after the production of themalized excitations. The account for energetic Auger- and delta-electrons result in the change of this distribution. The structure of the concentration distribution functions determines different scintillation decay kinetics and corresponding yield at different stages of the scintillation and from different parts of the track.

Source of strong fluctuations of spatial distribution of excitations in track region.

Classical estimations of different terms in energy resolution formula are based on statistical approach, which means that all terms are the result of large amount of events in each track. If we speak about energy resolution for energies of ionizing particle about tens and hundreds of electronvolts, one have to pay attention on relatively rare events in track which significantly change the track structure, the decay kinetics and the number of emitted photons. There are at least two examples of such significant events. The track topology is changed seriously if energetic Auger electrons with energies in keV region are emitted after ionization of deep core levels. Let us look in Fig. 1 where partial

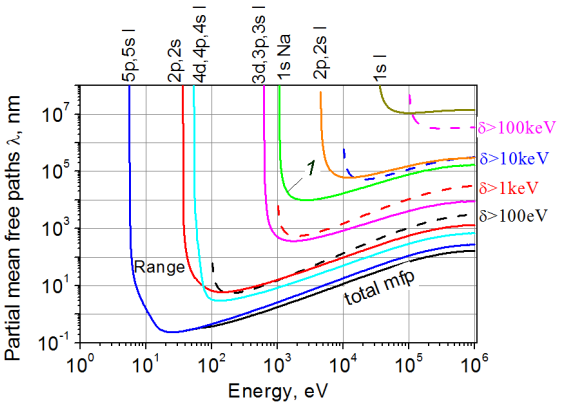

Fig. 1. Partial mean free paths for production of deep core holes (solid lines) at different core levels and energetic δ-electrons (dashed lines) as functions on energy of primary electron. The range of electron in the media is shown by solid green (*1*) curve.

mean free paths for ionization of different core levels in NaI are plotted as function of energy of ionizing particle together with the total range dependence on the primary energy of ionizing electron. The events below this line occur several times along the track length, whereas events above this line occur once per few tracks.

The same effect occurs when energetic δ-electrons are produced. Figure 1 shows the mean free path for production of δ-electrons with energy above certain energy. Again, the events below the range curve occur several times along the track length, whereas events above this line occur once per few tracks. In order to estimate the role of such rare events, we take two different topologies of the track and compare the response of the scintillator on these two events. One track is the track of 100 keV electron without branching, i.e. without emission of energetic secondaries. Another one is the track of three branches, each of which has initial energy about 30 keV.

Distribution of concentration of excitations in track regions.

The excitation density distribution can be calculated according to [4]. The main idea of this calculation is to calculate 1D distribution of secondary excitations along the track according to $-dE/dx$ stopping power with account for 3D thermalization of excitations. Thermalization stage describes the spread of secondary excitations due to diffusion accomplished with phonon emission, and the thermalization length depends on initial kinetic energy of secondary

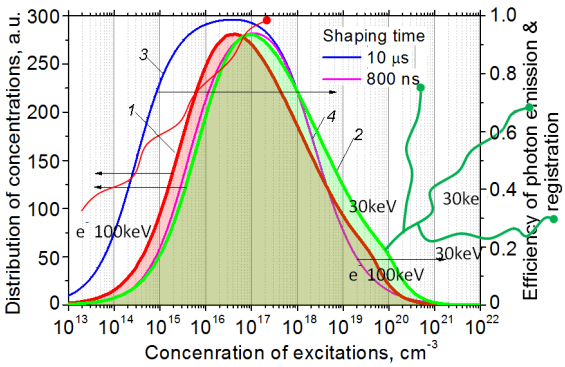

Fig. 2. Histogram of distribution of concentrations $w(\log n)$ in track region for 100 keV electron track in YAG without branching (red curve (*1*)) and with three branches (green curve (*2*)) for logarithmically distributed bins (left axis). Efficiencies of photon emission and detection $F(n)$ for two shaping times Δt (blue curve (*3*) — 10 μs, violet curve (*4*) — 800 ns) for the model expressed by Eq.(1) for $b_{ex\text{-}ex}n_{inter} = \tau_{ex}^{-1}$, $\tau_{ex} = 60$ ns, $n_{inter} = 10^{16}$ cm^{-3}, $g_{eh} = 20b_{ex\text{-}ex}$ (right axis).

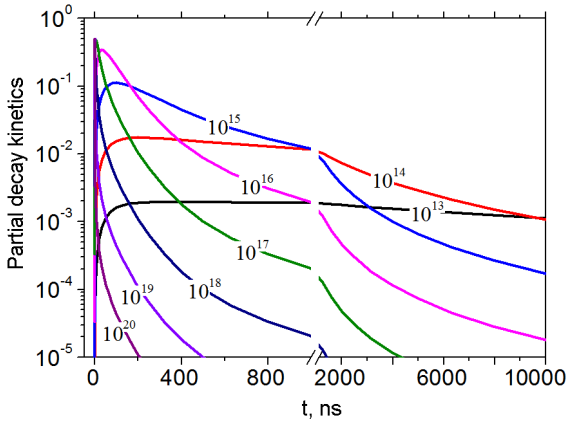

Fig. 3. Decay curves for emission from regions with different initial concentrations (shown in labels) for the model expressed by Eq. (1) for $b_{ex\text{-}ex}n_{inter} = \tau_{ex}^{-1}$, $\tau_{ex} = 60$ ns, $n_{inter} = 10^{16}$ cm^{-3}, $g_{eh} = 20b_{ex\text{-}ex}$.

electrons, phonon frequencies and parameters of carriers such as their mass (more exactly group velocity versus kinetic energy), density of states and electron-phonon interaction rate. After the convolution of 1D distribution of excitations along the track with 3D distribution after thermalization one can calculate the histogram of the local concentration of excitations around each excitation. This histogram calculated for logarithmically distributed bins $w(\log n)$ is shown by red (*1*) curve in Fig. 2 for parameters typical for YAG (stopping power is taken for YAG, energy of longitudinal phonon equal to 0.1 eV). The curve shows, for example, that the number of excitations surrounded by excitations with concentration from 10^{16} to $2{\cdot}10^{16}$ cm^{-3} is more than two times exceeds the number of excitations with concentration from 10^{15} to $2{\cdot}10^{15}$ cm^{-3} or from 10^{19} to $2{\cdot}10^{19}$ cm^{-3}. The peak of this distribution corresponds to $4{\cdot}10^{16}$ cm^{-3}. Only about 5 % of excitations are surrounded by high concentration above 10^{20} cm^{-3} or by low concentration below 10^{14} cm^{-3}.

If the track consist of say three branches, the distribution of the density of excitations $w(\log n)$ changes. We analyze the case when the track is branched at the very beginning, and the thermalization length is much less than the lengths of each branch. In this case the distribution is simply triple of the distribution for 33 keV track. This distribution is shown by green curve (10^{17}) in Fig. 3. We see that $w(\log n)$ is shifted by to higher densities in comparison with single branch track. The maximum of the distribution is at 10^{17} cm^{-3} instead of $4{\cdot}10^{16}$ cm^{-3}.

Nevertheless, the total number of excitations $N_{excitations} = \int w\log(n)d(\log n)$ is the same for both track topologies, so the number of emitted and detected photons $N_{photons}$ and therefore statistical term in energy resolution could be expected as the same. This conclusion is correct if we suppose that each excitation result in photon emission and all photons are detected.

Unfortunately this is not the case. The excitations in the region with high concentration could decay nonradiatively. This phenomenon is well-known and is accounted in most models of scintillation starting from the paper of Birks [5] and Murray [6] and in more recent papers (see, e.g. [7]). For charged carriers Auger processes involving neighbor electrons and holes could result in the disappearing of carriers (this process is 3rd order process on the concentration of electrons or holes). Neutral excitations like excitons, either free or self-trapped, can interact with each other and disappear in this process. The latter process is the 2nd order process on concentration of excitons. Therefore region of high concentration of excitations is characterized by partial transformation of excitations into scintillation photons, and the photon emission yield decreases rapidly with increase of concentration of excitations. The decay of

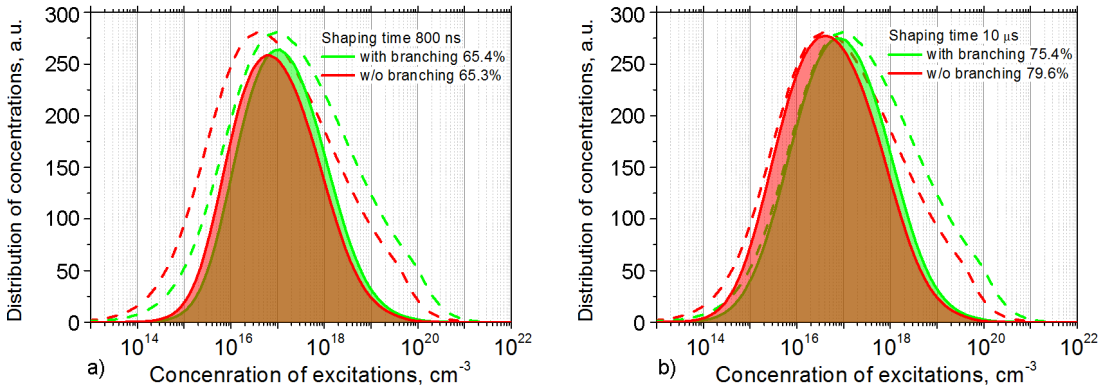

Fig. 4. Overlapping of $w(\log n)$ and $F(n)$ for two shaping times 800 ns (left panel) and 10 μs (right panel) for two topologies of electron track shown in Fig. 2: without branching (red) and with branching (green). Dashed curves show histograms of distribution of concentrations $w(\log n)$ for these topologies.

emission from these regions also modified and is characterized by accelerating at initial stages.

The regions with low concentration of electrons and holes are characterized by delayed recombination. The photon emission in this region results from bi-molecular recombination of carriers, and is characterized by long hyperbolic decay of emission. The decay becomes much longer with decrease of concentration. Photons emitted after the gate (shaping) time for registration of scintillation have no chance to be detected. Therefore again not all excitations from this region result in detected photons.

Some qualitative results can be found for rather simple analytically solvable set of equations studied in [8]. This model preserves the most important features of more complicated case, such as appearance of raise time for the response, fast initial stage of response and long emission components. The uniform distribution of excitations (excitons with concentration n_{ex} and holes and electrons with equal concentrations $n_h = n_e$) is considered. No Auger recombination terms are included. The set of equations includes only second order terms and can be written as:

$$\frac{dn_{ex}(t)}{dt} = \\ = -a_{ex}n_{ex}(t) - b_{ex-ex}n_{ex}^2(t) + g_{eh}n_e(t)n_h(t), \quad (1)$$
$$\frac{dn_e(t)}{dt} = -g_{eh}n_e(t)n_h(t), \quad n_e(t) = n_h(t).$$

The equation for excitons describes radiative recombination with coefficient $a_{ex} \equiv \tau_{ex}^{-1}$, τ_{ex} is the exciton radiation time, quadratic term corresponding to exciton-exciton annihilation with rate coefficient b_{ex-ex}, and bi-linear term describing the recombination of electrons and holes into excitons with rate coefficient g_{eh}. For electrons and holes we take into account only bi-linear process, part of which result in production of excitons. Therefore this model includes one radiative channel (for excitons) and one quenching process due to exciton-exciton non-radiative quenching. The equations should be accomplished by initial conditions for total concentration of excitations created after thermalization n^0. Here we suppose that all excitations are created as electron-hole pairs and no excitons are directly created. We use here term "excitons" but all other neutral excitations can be treated in the same manner.

This equation can be solved in terms of modified Bessel functions similar to the solution presented in [8]. We can introduce the critical concentration n_{inter} as the concentration of excitons at which the rate of the exciton-exciton interaction equals to the radiative time: $b_{ex-ex}\ n_{inter} = a_{ex}$. Here we choose $\tau_{ex} = 60$ ns, $n_{inter} = 10^{16}$ cm^{-3}. The electron-hole recombination constant is chosen equal to $g_{eh} = 20b_{ex-ex}$. The parameters taken for this example give satisfactory agreement with YAG:Ce^{3+} decay kinetics for excitation by 622 keV γ-quanta and 30 keV X-ray excitation [9]. The radiation time is taken not for excitons but for Ce^{3+} decay. We believe that we can use the proposed model in this case, since excitons are the intermediate excitations which pass the energy to Ce^{3+} impurity center.

Decay curves from regions with different concentration.

Decay curves for excitonic emission representing typical cases are shown below in Fig. 3 for different concentrations n^0. Decay curves for low concentrations $n^0 < n_{inter}$ are characterized by relatively long raise time and long hyperbolic decay tail. Both these parameters are sensitive to the initial concentration n^0, especially length of the decay tail. For higher concentrations $n^0 > n_{inter}$ there is no detectable raise time, and decay becomes much faster than exponential one characterized by radiation time τ_{ex}. The acceleration of the decay increases with increase of local concentration of excitations n^0.

Fluctuations of phonon emission and detection efficiency and decays due to track branching.

The efficiency of emission and detecting scintillation photons $F(n)$ can be calculated using this model for different shaping time, 800 ns and 10 μs. These two curves are plotted as functions of local concentration of excitations n^0 in Fig. 2 (blue and violet curves, right axis). The efficiency of emission of photons drops with increase of n^0 when $n^0 > n_{inter}$ independently on shaping time. On contrary, for $n^0 < n_{inter}$ the decrease of efficiency of detecting of phonons depends strongly on the shaping time, for shorter shaping time the decrease starts at higher concentrations.

Figure 4 shows the result of multiplying of $F(n)$ by the plotted in Fig. 2 histograms w log(n) of concentrations for two topologies of track without branching (red curves) and with triple branching (green curves). The sum of these products over histogram bins $N_{photons} = \int w(\log n)F(n)d(\log n)$ gives the total efficiency of registration of scintillating photons. The histograms w(log n) are shown by dashed curves. The comparison of figures for 800 ns shaping time (left panel) with 10 μs shaping time shows that for gates of 10 μs about all photons from regions of concentration between 10^{15} and 10^{17} cm^{-3} are registered, whereas for gates of 800 ns significant fraction of photons from regions with concentration less than 10^{16} cm^{-3} are missed.

The calculation of the number of emitted and detected photons in our example for 800 ns gate gives about the same result for both track topologies: $N_{photons}/N_{excitations} =$ 0.653 for track without branches and 0.654 for track with branches, the difference is 0.1 %. In this particular case the shift of density distribution to higher concentrations for track with branches result in lower efficiency of emission of photons from high density regions and higher detection probability of photons from low density regions due to shortening of decay. The resulting difference between two tracks is small. The result for 10 μs shaping time is more surprising: $N_{photons}/N_{excitations} =$ 0.796 for track without branches and 0.754 for track with branches, the difference is 5 %. In this case the shaping time is long enough to detect more photons from low concentration region, and the decrease of efficiency of emission of photons from high density regions is not compensated. Therefore we can conclude that this difference could result in significant deterioration of energy resolution. The result that the photon yield fluctuate more for 10 μs shaping time in comparison with 800 ns one is not general and depends on how functions w(log n) and $F(n)$ are overlapped.

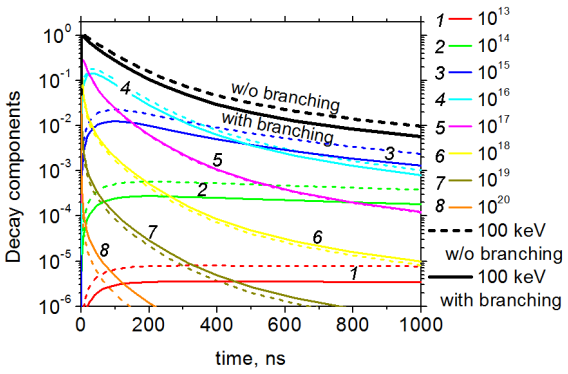

Fig. 5. Decay curves for emission from regions with different initial concentrations (shown in labels) with account for the fraction of corresponding concentration and total decay curves (black curves) for track without branching (dashed) and with branching (solid).

The analysis of curves presented in Fig. 2 shows that the compensation of fluctuations of track branching is possible if the middle points of low-concentration slopes of w(log n) and $F(n)$ correspond to similar concentrations.

The decay curves for the discussed two topologies of tracks are plotted in Fig. 5 (black solid and dashed curves for track with branching and without branching, correspondingly) together with inputs to these curves from regions with different concentrations weighted with w(log n) functions.

The track without branching is characterized by larger contribution of slow components, slower decay at initial stages and even appearance of some raising time.

The dependence of the decay on the track topology could serve as a physical background for the method of improving of energy resolution proposed in [10]. In this investigation the way to improve the energy resolution using digital pulse shape analysis and weighting of signals for three time windows is proposed. Our study shows that the regions with different density of excitations give the specific input to overall decay profile.

Role of shallow traps in fluctuations of phonon emission and detection efficiency

The rate of exciton-exciton interaction resulting in quenching in regions with high concentration of excitations seems to be intrinsically property of the host material. Therefore high-density slope of the efficiency curve $F(n)$ could not be changed. On contrary, the low-density slope of $F(n)$ could be modified. This slope is connected with long component of the decay, and therefore on the rate of electron-hole recombination. The bi-molecular rate of the *e-h* recombination is controlled mainly by the diffusion coefficients of charge carriers, which in turn depend on shallow traps for electrons and holes. The concentration of shallow traps can be changed by growth conditions and by incontrollable impurities, which modify long components of the decay. In the previous example we use the value $g_{eh} = 20b_{ex\text{-}ex}$. Figure 6 shows the influence of emission and detection efficiency curve $F(n)$ on the value g_{eh}. In case of higher concentration of shallow traps (and therefore lower recombination rate and lower mobility of carriers, $g_{eh} = 5b_{ex\text{-}ex}$) the curves $F(n)$ for two shaping times are shown as dashed curves. In case of lower concentration of shallow traps (and therefore higher recombination rate and higher mobility of carriers, $g_{eh} = 80b_{ex\text{-}ex}$) the curves $F(n)$ are shown as dash-dotted curves. We see that the low-concentration slope of the emission and detection efficiency curve $F(n)$ strongly depends on the recombination rate. Energy resolution deterioration due to branching of tracks depends on the position of the middle of this slope relative to the middle of the slope of $w(\log n)$ function, as we mention above. The compensation of fluctuations of track branching is possible if the middle points of low-concentration slopes of $w(\log n)$ and $F(n)$ correspond to similar concentrations. Therefore the proper control of the mobility of charge carriers due to the presence of shallow traps could minimize the additional terms in energy resolution estimations arisen by different track topologies.

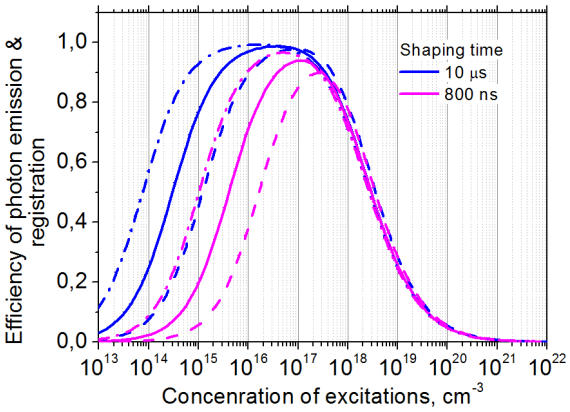

Fig. 6. Efficiencies of photon emission and detection $F(n)$ for two shaping times Δt (blue curves — 10 μs, violet curves — 800 ns) for the model expressed by Eq. (1) for $g_{eh} = 5b_{ex\text{-}ex}$ (dashed curves), $g_{eh} = 20b_{ex\text{-}ex}$ (solid), $g_{eh} = 5b_{ex\text{-}ex}$ (dash-dotted), $b_{ex\text{-}ex}n_{int\ er} = \tau_{ex}^{-1}$, $\tau_{ex} = 60$ ns, $n_{inter} = 10^{16}$ cm^{-3}.

4. Conclusions

We discuss the role of relatively rare scattering events, namely creation of high energy Auger electrons after excitation from L- and K-levels and creation of high energy δ-electrons, in the change of track branching and therefore the modification of distribution of concentrations of excitations in the track region. This distribution is shifted toward higher concentrations in case of track branching, and therefore the number of emitted and detected photons deviates significantly depending of the shaping time of the signal detection. This can be a reason for deterioration of energy distribution. Simultaneously with the change of distribution of excitation the inputs to the decay curve also changed. Therefore the digital pulse shape analysis for each scintillation event together with weighting of signals from different time windows can provide a way to correct scintillation signal and improve the energy resolution, as it is proposed in [10]. It is also demonstrated that the deterioration of energy resolution due to the effect of track branching depends on the transport properties of electrons and holes before recombination. Therefore the shallow traps which change the mobility of

charge carriers could influence the long components of the decay and therefore modify the input to scintillation signal from regions with low concentration of excitations. This effect could be significant in deterioration of energy resolution of scintillators.

Acknowlegements. ANV thanks the support by the Ministry of Education and Science of the Russian Federation (state contract No. RFMEFI61614X0006).

References

1. I.V.Khodyuk, S.A.Messina, T.J.Hayden et al., *J. Appl. Phys*., **118**, 084901 (2015).
2. K.Yang, P.R.Menge, *J. Appl. Phys*., **118**, 213106 (2015).
3. M.Moszynski, A.Syntfeld-Kazuch, L.Swiderski et al., *Nucl. Instr, Meth. Res. A*, **805**, 25 (2016).
4. A.N.Vasil'ev, in "Engineering of Scintillation Materials and Radiation Technologies", ed. by A.Gektin and M.Korzhik, Springer Proc. in Physics 200 (2018), ch.1.
5. J.B.Birks, Theory and Practice of Scintillation Counting, Pergamon, New York (1964).
6. R.B.Murray, A.Meyer, *Phys. Rev*., **112**, 815 (1961).
7. W.W.Moses, G.A.Bizarri, R.T.Williams et al., *IEEE Trans. Nucl. Sci*., **59**, 2038 (2012).
8. G.Bizarri, W.W.Moses, J.Singh et al., *J. Luminescence*, **129**, 1790 (2009).
9. A.Belsky, private communication
10. A.Gektin, S.Vasyukov, V.Gayshan et al., in: Proc. of 14th Intern. Conf. on Scintillating Materials and their Applications, Chamonix, France (2017).